Progress in Heavy-Quark Physics from BaBar, Belle, and CLEO

Jeffrey D. Richman

Department of Physics
University of California
Santa Barbara, CA 93106

Abstract. I present an overview of progress in heavy-quark physics, focusing on results from e^+e^- colliding-beam experiments. The central goal of these experiments is to discover and precisely measure CP asymmetries in a variety of processes in the B-meson system. Together with related quantities, such as the magnitudes of Cabibbo-Kobayashi-Maskawa elements, these measurements will overconstrain the Standard-Model framework for CP violation, either confirming this framework or providing evidence for new physics. The heavy-quark physics program also includes many other fascinating processes that do not bear directly on CP violation but which nevertheless are of great interest. Such processes as electroweak penguin decays, rare hadronic B decays, and $D^0-\bar{D}^0$ mixing have sensitivity to new physics or help to sharpen our understanding of physics within the Standard Model. I also discuss the new B-factory accelerators, whose remarkable success should ensure rapid progress in this field. My presentation is intended to highlight some of the most interesting aspects of the subject for nonexperts.

INTRODUCTION

I am delighted to speak to this audience of nuclear and particle physicists on recent progress in heavy-quark physics. My talk focuses on the program of the three e^+e^- colliding-beam experiments—BaBar, Belle, and CLEO—all of which operate at a center-of-mass energy equal to the mass of the $\Upsilon(4S)$ resonance: $\sqrt{s} = 10.58$ GeV. The overwhelmingly dominant decays are $\Upsilon(4S) \rightarrow B^0\bar{B}^0$ and $\Upsilon(4S) \rightarrow B^+B^-$, which provide a clean and kinematically constrained means to produce B mesons. Charm mesons are also produced at this energy, both as daughter particles of B mesons and from the continuum process $e^+e^- \rightarrow c\bar{c}$.

The CLEO experiment, which runs at the Cornell Electron Storage Ring (CESR), has a mature and ongoing heavy-quark physics program, while BaBar (at SLAC) and Belle (at KEK) are just beginning theirs. These new experiments operate at e^+e^- storage rings that have unequal beam energies, so that the resulting $B\bar{B}$ system is boosted relative to the detector. As we will see, this feature enables BaBar and Belle to measure time-dependent CP asymmetries in the neutral B meson system. First results from BaBar and Belle will be presented later this summer, so at this point I can only present a status report on the rapid progress being made toward the CP asymmetry measurements. Most of the results I will present are from CLEO, although I will also describe some important measurements from the LEP experiments at CERN, which use the process $e^+e^- \to Z \to b\bar{b}$ to study a variety of b-hadrons. In a separate talk [1], Barry Wicklund will describe results on heavy-quark physics from the Fermilab hadron-collider experiments. Other related plenary-session talks are by Mohapatra [2] on CP violation and El-Khadra [3] on lattice QCD calculations.

The title—"Conference on the Intersections of Particle and Nuclear Physics"—raises the question of whether the fields of heavy-quark and nuclear physics do, in fact, intersect! One example can be written directly in the form of an equation,

$$|V_{ud}|^2 + |V_{us}|^2 + |V_{ub}|^2 = 1, \tag{1}$$

which ties together measurements of V_{ud} and V_{ub}. The value of $|V_{ud}|$ is extracted from superallowed β decays of nuclei, while $|V_{ub}|$ is obtained from semileptonic decays of the B meson. More generally, both nuclear and heavy-quark physics have long focussed on the issues of discrete symmetries and their violation; today, searches for CP and T violation by physicists in both fields provide complementary approaches to these profound questions.

I will begin with an overview of the goals and ideas of heavy-quark physics and then describe the experiments and accelerators operating at the $\Upsilon(4S)$. I then discuss progress in four main areas: semileptonic decays and measurements of the Cabibbo-Kobayashi-Maskawa (CKM) matrix elements V_{cb} and V_{ub}; rare B decays, including electroweak and hadronic penguins; mixing in the $D^0\bar{D}^0$ system; and searches for CP asymmetries in B decays. First results on CP asymmetries from BaBar and Belle will be available later this summer, so I will simply present a status report on these experiments. (In the interests of full disclosure I should say that I am a member of the BaBar collaboration and a former member of the CLEO collaboration!)

GOALS AND IDEAS OF HEAVY-QUARK PHYSICS

The most compelling question in heavy-quark physics is whether the source of CP violation lies within the Standard Model, in physics beyond it, or in some combination of the two. The Standard Model can accomodate precisely one CP-violating (or "weak") phase, which resides in the three-generation CKM quark mixing matrix

$$V = \begin{pmatrix} V_{ud} & V_{us} & V_{ub} \\ V_{cd} & V_{cs} & V_{cb} \\ V_{td} & V_{ts} & V_{tb} \end{pmatrix} = \begin{pmatrix} 1-\frac{1}{2}\lambda^2 & \lambda & A\lambda^3(\rho - i\eta) \\ -\lambda & 1-\frac{1}{2}\lambda^2 & A\lambda^2 \\ A\lambda^3(1-\rho-i\eta) & -A\lambda^2 & 1 \end{pmatrix} + \mathcal{O}(\lambda^4). \tag{2}$$

Here we have used the Wolfenstein parametrization, which shows explicitly that there are only four independent real parameters needed to specify the matrix. The expansion parameter is $\lambda = \sin\theta_C \approx 0.22$. The weak phase in the CKM matrix can manifest itself in many different ways, leading to CP asymmetries both small and large.

CP violation was discovered in 1964 in the neutral kaon system by Christensen, Cronin, Fitch, and Turlay [4], who observed the mode $K_L^0 \to \pi^+\pi^-$ with a branching fraction of around 10^{-3}. Jim Cronin made some prescient remarks in his Nobel-prize lecture [5]:

> ...the effect [of CP violation] is telling us that at some tiny level there is a fundamental asymmetry between matter and antimater, and it is telling us that at some tiny level interactions will show an asymmetry under the reversal of time. We know that improvements in detector technology and quality of accelerators will permit even more sensitive experiments in coming decades. We are hopeful, then, that at some epoch, perhaps distant, this cryptic message from nature will be deciphered.

In the B system, the Standard Model predictions for CP asymmetries are not at the 10^{-3} level, but in the range 0.1 to 1. This doesn't mean that they are easy to measure, because they are associated with decay processes that typically have small branching fractions, in the range 10^{-4} to 10^{-5}. Nevertheless, the outstanding feature of the B meson system is that the observed CP asymmetries may well be quite large.

Let's examine the conditions [6,7] required to produce a CP asymmetry in a decay process. First, we need a decay involving (at least) two amplitudes, A_1 and A_2, one of which has a CP-violating phase ϕ_2, which we explicitly display as $A_2 = a_2 \exp(i\phi_2)$. The total amplitude is given by

$$A = A_1 + a_2 e^{i\phi_2}. \tag{3}$$

Initially, we assume that A_1 and A_2 have no relative CP-*conserving* phase; A_1 and a_2 are therefore relatively real. Because overall phases do not affect the rate, we can take A_1 and a_2 to be real. The amplitude for the CP-conjugate (antiparticle) process is

$$\bar{A} = A_1 + a_2 e^{-i\phi_2}, \tag{4}$$

up to an overall phase [7]. It is easy to show that $|A| = |\bar{A}|$. *Thus, even though a CP-violating phase ϕ_2 is present, and the rates for both processes are affected by the value of ϕ_2, without a relative CP-conserving phase there is no CP asymmetry.*

We next introduce a CP-conserving phase (δ_2) in addition to the CP-violating phase. The total amplitudes for the original and CP-conjugate processes (up to an overall phase) are

$$A = A_1 + a_2 e^{i(\phi_2+\delta_2)} \qquad \bar{A} = A_1 + a_2 e^{i(-\phi_2+\delta_2)}. \tag{5}$$

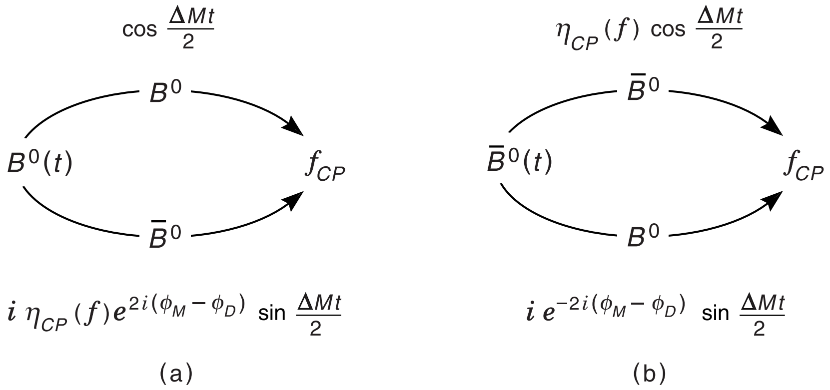

FIGURE 1. The interference between $B^0\bar{B}^0$ mixing and decay can be used to study CP asymmetries. The meson, a initially a B^0 or $\bar{B}^0$, is tagged using correlations with other particles produced at the same time. Due to B^0-$\bar{B}^0$ oscillations, the initial state evolves (becoming $B^0(t)$ or $\bar{B}^0(t)$) and develops both B^0 and $\bar{B}^0$ components. The decays of these states to a common final state (f_{CP}) interfere, and the time-dependent rates $\Gamma(B^0(t) \to f_{CP})$ and $\Gamma(\bar{B}^0(t) \to f_{CP})$ differ due to the CP-violating phase in the interference term.

In this case, one finds that $|A| \neq |\bar{A}|$, so that the process will display a CP asymmetry. We therefore need to study decays in which there is interference involving *both* the weak phase of interest and a well understood CP-conserving phase. Unfortunately, it is not yet possible to calculate phases due to strong final-state interactions. Even though so-called "direct CP violation" (from the interference between two direct decay amplitudes) can be quite interesting, it is therefore not the best source of information on weak phases.

However, a well understood CP-conserving phase arises from particle-antiparticle oscillations, or mixing. Figure 1 shows how we can use the interference between mixing and decay to study CP violation in B^0 decay. This method leads to *time-dependent* CP asymmetries. Mixing is especially interesting because it is sensitive to virtual intermediate states that can introduce weak phases other than those expected in the Standard Model. We note that the CP violation "in mixing" observed in the $K^0\bar{K}^0$ system arises from the interference between mixing amplitudes through real and virtual intermediate states. In the $B^0\bar{B}^0$ system, the contribution to mixing from real intermediate states is very small, and the CP asymmetry from mixing alone is expected to be difficult to measure.

The Standard Model framework for CP violation is specific and predictive, and it is possible in principle to infer the level of CP asymmetries from measurements of CP-*conserving* observables. In particular, the unitarity of the CKM matrix leads to six relations of the form

$$V_{ud}V_{ub}^* + V_{cd}V_{cb}^* + V_{td}V_{tb}^* = 1, \tag{6}$$

where in this case we have taken the inner product between the first and third column of the matrix. This equation can be represented graphically as the so-called unitarity triangle, whose area is a direct measure of CP violation in the Standard Model. The B system is special in that each of the three terms in Eq. 6 is of order λ^3, leading to a triangle that is not as flat as those from the other five relations, and it means that the CP asymmetries are expected to be larger. The triangle can be specified by measurements of the lengths of the sides alone (non-CP-violating observables) or by measurements of angles between the sides (CP violating observables). (The overall orientation of the triangle is non-physical and depends on the convention used for the quark phases.) Thus, a second major goal of heavy-quark physics is to measure the magnitudes of CKM elements, partly to pin down all the parameters of the Standard Model, but also to achieve a comprehensive understanding of CP violation and its connection to the CKM matrix. Measurements of semileptonic decays, $B^0\bar{B}^0$ and $B_s\bar{B}_s^0$ oscillation rates, and the electroweak penguin processes $b \to tW^- \to s(d)$ provide information on $|V_{cb}|$, $|V_{ub}|$, $|V_{td}|$, and $|V_{ts}|$.

CP asymmetries are measured in hadronic processes, where the necessary interference terms are present in the Standard Model. Because the *phases* of CKM matrix elements are extracted from asymmetries rather than decay rates, the hadronic matrix elements can cancel, removing the dependence on theory. In contrast, to extract the *magnitudes* of CKM elements, we measure decay rates and rely on theoretical calculations that predict each rate up to an unknown overall constant, which is the CKM factor. For example, the branching fraction for a semileptonic decay of a meson M with quark content $Q\bar{q}$ can be expressed in the form

$$\mathcal{B}(M_{Q\bar{q}} \to X_{q'\bar{q}}\ell\bar{\nu}) = \gamma_{\text{theory}}|V_{q'Q}|^2\tau_M. \tag{7}$$

Experimentalists measure the branching fraction and lifetime τ_M, while theorists must predict γ_{theory}. Note that the relative error on $|V_{q'Q}|$ is half that on the branching fraction due to the square root; this helps to make poor results look better! The processes used to extract the magnitudes of CKM elements are sufficiently simple that it is possible to make theoretical predictions for the decay rates with a precision typically in the 10% to 50% range in the rate, or in the 5% to 25% range for the magnitude of the CKM element.

The need to calculate the factor γ_{theory} and other related quantities has led to an intensive effort, both theoretical and experimental, to better understand the dynamics of processes involving heavy quarks. This represents a third major area of research in heavy-quark physics. There have been long-running programs of measuring and calculating form factors for semileptonic decays, decay constants for leptonic decays and mixing, and the rates for electroweak penguins. Sophisticated methods such as Heavy Quark Effective Theory (HQET) [8] and lattice QCD [3] are being used to constrain or predict various hadronic parameters. The relatively large masses of the bottom and charm quarks (compared to Λ_{QCD}) have been key to achieving advances in these calculations.

Although it has not been possible to carry out comparable calculations of the decay rates for hadronic final states, there has nevertheless been a recent effort to extract useful CKM information from hadronic decay rates. In this approach,

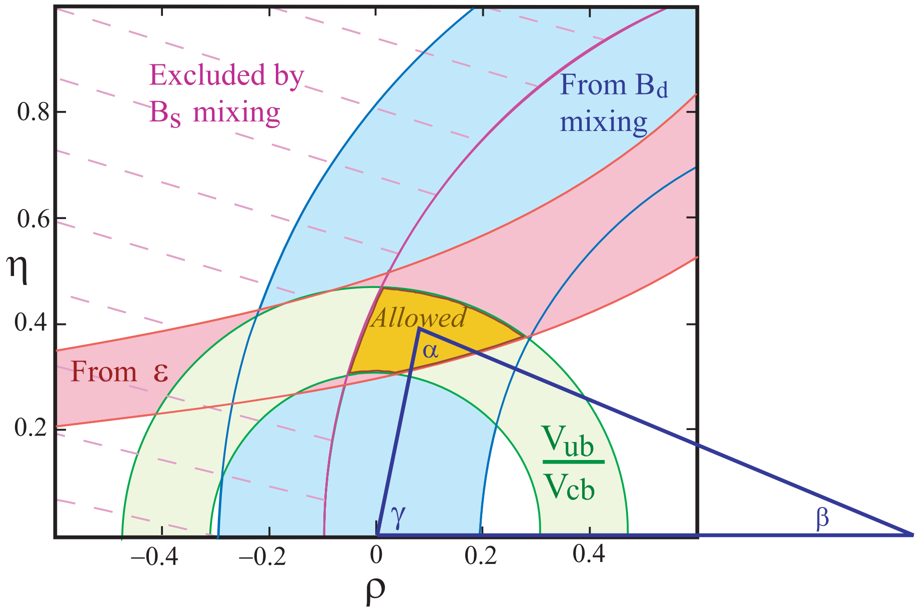

FIGURE 2. Constraints on the ρ-η plane from different types of measurements. The lengths of the sides are determined from rates for semileptonic decays, $B^0\bar{B}^0$ mixing, and $B_s\bar{B}_s$ mixing. Measurements from kaon physics can also supply important constraints, as in the quantity ϵ from CP violation in the $K^0\bar{K}^0$ system. Current investigations of CP asymmetries will determine the angles of the triangle α, β, and γ. When the constraints are combined statistically, the sharp corners are rounded off. (Figure used with permission of S. Stone.)

measurements are used to constrain the unknown hadronic parameters as much as possible.

Finally, heavy-quark decays involving loops are a fourth major area of investigation. Such processes, which include the electroweak penguins already mentioned, can be affected by new heavy particles that circulate in the loops. I will review some of the progress made in these studies, including the important case of $D^0\bar{D}^0$ mixing. This process is expected to be highly suppressed in the Standard Model due to GIM cancellations, and it provides a particularly sensistive way to search for the effects of new physics.

EXPERIMENTS AND ACCELERATORS AT THE $\Upsilon(4S)$

The success of the B factories running at the $\Upsilon(4S)$ resonance has been a remarkable achievement by the accelerator-physics community. These are the highest luminosity colliding-beam machines in the world! There are many complex problems that have been solved in the design of such machines, which involve extremely high-current, multi-bunch operation. The PEP-II ring, for example, is designed to store 1658 particle bunches in each beam; the issues of multibunch instabilities and the avoidance of parasitic crossings (bunch crossings not at the interaction

TABLE 1. Parameters of accelerators operating at the $\Upsilon(4S)$. The integrated luminosities of BaBar and Belle are given as of August 2000. For all experiments, the integrated luminosity includes both on-$\Upsilon(4S)$ and off-resonance (continuum) running.

Machine	CESR	PEP-II	KEKB
Detector	CLEO	BABAR	Belle
Date 1st events recorded	1979	May '99	June '99
Circumference (km)	0.768	2.199	3.016
Number of Rings	1	2	2
E_{e^+} (GeV)	5.3	3.1	3.5
E_{e^-} (GeV)	5.3	9.0	8.0
$\beta\gamma$	0.06 (B)	0.56 ($\Upsilon(4S)$)	0.42 ($\Upsilon(4S)$)
Num. of beam bunches (design)	$9 \times 4 \rightarrow 9 \times 6$	1658	2700
I_{beam} (A) (design)	$0.26 \rightarrow 0.5$	2.16 (e^+), 1.0 (e^-)	2.6 (e^+), 1.1 (e^-)
Δs_{bunch} (m) (design)	4.2	1.26	1.2
Δt_{bunch} (ns) (design)	14	4.2	4.0
Beam crossing angle (mrad)	± 2.1	0 (magnetic sep.)	± 11
Achieved luminosity cm^{-2}s^{-1}	8.3×10^{32}	$\sim 2 \times 10^{33}$	$\sim 2 \times 10^{33}$
Best daily integ. lum. (pb^{-1})	140	90	40
Integrated luminosity (fb^{-1})	13	14.8	6.8

point) are extremely important. These machines must store very high beam currents, while at the same time maintaining tolerable background conditions for the detectors, and there are stringent requirements on the vacuum quality.

Table 1 summarizes some of the main features of CESR, KEKB, and PEP-II. CESR has operated for many years and has produced a long series of results in B physics going back to the first observation of exclusive B meson decays. The electron and positron beams are at equal energy, so the $\Upsilon(4S)$ is produced at rest in the lab frame, and the daughter B mesons from $\Upsilon(4S) \rightarrow B\bar{B}$ have very low velocity: $\beta\gamma \approx 0.06$. Each beam (electrons or positrons) consists of 9 bunch trains with 4 bunches each, for a total of 36 bunches. To avoid parasitic collisions, the beams are put into special "pretzel" orbits that weave around each other with transverse displacements of up to 2 cm from the centerline of the accelerator vacuum chamber.

PEP-II and KEKB are only a year old, but already they have reached unprecedented beam currents and luminosities. Because these machines store beams at unequal energies, they require separate rings for electrons and positrons, except for a complicated region around the interaction point where the beams intersect. As a benefit, parasitic beam crossings are an issue only in the interaction region itself. Successive arriving beam bunches are 4.2 ns (1.26 m) apart (with 1658 bunches/beam) in PEP-II, and to prevent an outgoing bunch from interacting with the next incoming bunch, the beams are deflected with dipole magnets starting about 20 cm from the interaction point. In KEKB a different approach is taken, where the beams enter and exit with a ± 11 mrad crossing angle.

PEP-II has achieved a peak luminosity $\mathcal{L} = 2.3 \times 10^{33}$ cm^{-2}s^{-1} with total beam currents of $I_{e^-} = 0.75$ A and $I_{e^+} = 1.3$ A, and 606 bunches/beam. KEKB has achieved nearly the same luminosity with 1146 bunches per beam. At $\mathcal{L} = 3 \times 10^{33}$ cm^{-2}s^{-1}, BaBar and Belle will each accumulate about 30 million $\Upsilon \to B\bar{B}$ events in 10^7 s. All three machines—CESR, KEKB, and PEP-II—should reach even higher luminosities in the future.

SIMPLE PROCESSES: SEMILEPTONIC DECAYS AND MAGNITUDES OF CKM ELEMENTS

Semileptonic B decays are sufficiently simple to allow us to extract the magnitudes of CKM elements from decay rates. Strong interaction effects are, of course, still present, but they are isolated to a single hadronic current that can be rigorously parametrized by form factors. The form factors are Lorentz-invariant functions of q^2, the square of the mass of the virtual W.

Because semileptonic decays produce three-body final states (at least), there is a range of allowed kinematic decay configurations, whose population in the Dalitz plot of q^2 vs. E_ℓ (lepton energy) provides detailed information on the decay dynamics. For any semileptonic decay $B \to X\ell^-\bar{\nu}$, q^2 characterizes the recoil velocity of the hadronic daughter system X, since

$$w \equiv \gamma_X = \frac{E_X}{m_X} = \frac{M_B^2 + m_X^2 - q^2}{2M_B m_X}. \tag{8}$$

At maximum q^2 ($q^2_{\rm max} = (M_B - m_X)^2$), $w = 1$, and the daughter hadron has zero recoil velocity relative to the B.

There are two main classes of semileptonic B decays, the dominant $b \to c\ell^-\bar{\nu}$ modes, which can be used to extract $|V_{cb}|$, and the much rarer and more difficult to study $b \to u\ell^-\bar{\nu}$ decays, which are used to determine $|V_{ub}|$. There is a large difference in how well we understand these two types of decays. The main $b \to c\ell^-\bar{\nu}$ modes, $B \to D^*\ell^-\bar{\nu}$ and $B \to D\ell^-\bar{\nu}$, have been studied in some detail; together they represent a substantial fraction (about two-thirds) of the inclusive semileptonic rate ($B(B \to Xe\nu) = (10.5 \pm 0.8)\%$) [9]. Form factors for these processes have been measured [11–13] by studying the kinematic distributions and their correlations, and their mild variation within the small kinematically accessible range of w (about 1 to 1.6) is consistent with theoretical expectations [8]. In contrast, the allowed range in w is typically much larger in $b \to u\ell^-\bar{\nu}$ transitions, so the recoil velocity of the daughter hadron can be quite large and the variation in the form factors much greater than for $b \to c\ell^-\bar{\nu}$ decays.

There has been a large effort, both experimental and theoretical, to extract $|V_{cb}|$ from the $B \to D^*\ell^-\bar{\nu}$ decay rate at zero recoil. At $w = 1$, a $B \to D^{(*)}$ transition produces very little disturbance to the hadronic wave function, since one heavy quark (b) is simply replaced by another (c), with little momentum transfer to the spectator quark. In the heavy-quark symmetry limit, $m_b, m_c \gg \Lambda_{\rm QCD}$, the meson

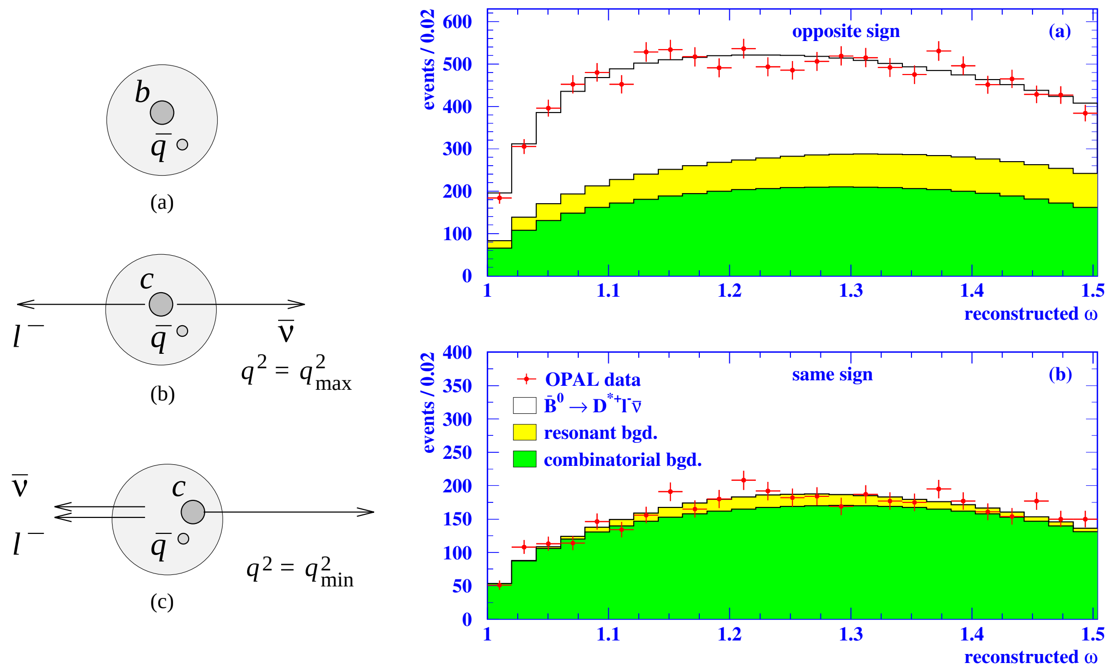

FIGURE 3. $B \to D^*\ell^-\bar{\nu}$ and the measurement of $|V_{cb}|$. The figures at the left show (a) a B meson before decay, (b) semileptonic decay configuration at high q^2 (low recoil velocity of daughter hadron), and (c) semileptonic decay configuration at low q^2 (high recoil velocity of daughter hadron). The goal of measurements is to determine $|V_{cb}|$ from the decay rate at high q^2, where the meson wave function is least disturbed and theoretical calculations are most reliable. The figures at right show OPAL data for $B \to D^{*+}\ell^-\bar{\nu}$ using a partial reconstruction technique for the D^{*+}. This technique gives a larger signal yield (and higher backgrounds) than the usual full reconstruction. The signal is seen in the opposite-sign lepton-D^* charge correlations (a) at right, while a test of the understanding of backgrounds is provided by the same-sign charge correlation data, shown in (b) at right. The rate is extrapolated to $\omega = 1$, where ω is the same as the quantity w discussed in the text.

is completely undisturbed by the decay. The decay rate can therefore be predicted with a relatively small uncertainty. (The decay $B \to D\ell^-\bar{\nu}$ has a smaller branching fraction, more background, and is forbidden by angular-momentum conservation at the zero-recoil point.) The differential decay rate for $B \to D^*\ell^-\bar{\nu}$ can be written

$$\frac{d\Gamma(B \to D^{*+}\ell^-\bar{\nu})}{dw} = \frac{G_F^2 M_B^5}{48\pi^3} K(w)|V_{cb}|^2 \mathcal{F}(w)^2, \tag{9}$$

where $w = E_{D^*}/m_{D^*}$) and $K(w)$ is a known kinematic function. The theoretical uncertainties are contained in $\mathcal{F}(w)$, which is a linear combination of the three form factors that govern the decay. Numerous estimates for $\mathcal{F}(1)$ have been made in the framework of heavy-quark effective theory (HQET) and in lattice QCD. One recent compilation made for Particle Data Group [9] gives $\mathcal{F}(w) = 0.93 \pm 0.05$, while another compilation [10] gives $\mathcal{F}(1) = 0.913 \pm 0.042$.

TABLE 2. Results on $|V_{cb}|$ from experiments at the $\Upsilon(4S)$ and the Z. From Ref. [16]. A recent new preliminary CLEO measurement is discussed in the text.

Mode	$\lvert V_{cb}\rvert$	Comment
$B \to D^{*+}\ell^-\bar{\nu}$ (from $Z \to bb$)	$0.0367 \pm 0.0023 \pm 0.0018$	$\mathcal{F}(w)$ param. from dispersion relations
$\bar{B} \to D^{*+}\ell^-\bar{\nu}$ (from $\Upsilon(4S)$)	$0.0392 \pm 0.0030 \pm 0.0019$	Linear $\mathcal{F}(w)$ param. + correction
$\Gamma(b \to c\ell^-\bar{\nu})$ (Z)	$0.0408 \pm 0.0005 \pm 0.0025$	B^0, B^+, B_s, b-baryons
$\Gamma(B \to X_c\ell^-\bar{\nu})$ $(\Upsilon(4S))$	$0.0400 \pm 0.0010 \pm 0.0024$	B^0, B^+ admixture

Experimentalists have attempted to measure the rate near $w = 1$, usually by performing a measurement over the full phase space and then performing an extrapolation to $w = 1$, guided by theoretical shapes. Figure 3 shows the w spectrum for $B \to D^*\ell^-\bar{\nu}$ decay measured by the OPAL experiment [14]. Table 2, taken from Ref. [16], compares the values of $|V_{cb}|$ obtained from several different methods. Heavy-quark expansion techniques have also been used by theorists to predict the inclusive semileptonic rate; these results are comparable in overall precision to those from $B \to D^*\ell^-\bar{\nu}$, although the experimental errors are somewhat smaller. An update [13] from CLEO for $B \to D^*\ell^-\bar{\nu}$ became available after this conference but is still based on only 3.3 M $B\bar{B}$ events. The preliminary results are $B(\bar{B}^0 \to D^{*+}\ell^-\bar{\nu}) = (5.66 \pm 0.29 \pm 0.33)\%$ and $|V_{cb}|\mathcal{F}(1) = 0.0424 \pm 0.0018 \pm 0.0019$.

The measurement of $|V_{ub}|$ is significantly more difficult. This quantity was first measured from the rate beyond the inclusive $B \to X_c\ell^-\bar{\nu}$ endpoint, but more recently it has been determined from measurements of $B \to \pi\ell^-\bar{\nu}$ and $B \to \rho\ell^-\bar{\nu}$ exclusive rates. Because the daughter quark in the $b \to u$ transition is light, the zero-recoil point of the daughter hadron does not provide a solid point for predicting the form factors. Recent results from CLEO [17] have been combined with an earlier study [18] and are summarized in Fig. 4, with the final value $|V_{ub}| = (3.25 \pm 0.14^{+0.21}_{-0.29} \pm 0.55) \times 10^{-3}$, where the errors are statistical, systematic, and theoretical. The $B \to \rho\ell^-\bar{\nu}$ signal yield is 216 ± 32 events. The measured branching fraction depends to some extent on which theoretical model is used to determine the experimental detection efficiencies, since the analysis uses cuts on the lepton energy and other quantities. An additional theoretical error on $|V_{ub}|$ arises from uncertainties in the theoretical predictions for the overall rate; this is now the dominant error for exclusive measurements. (It should be noted that the theoretical error quoted in the CLEO paper is not based on the spread among the $|V_{ub}|$ values, which is smaller.)

A third and very interesting approach to measuring $|V_{ub}|$ has been pursued by the LEP experiments, which can measure the $b \to u\ell^-\bar{\nu}$ rate inclusive rate over a reasonably broad region of phase space. Although these measurements have larger statistical errors, the theoretical uncertainties are reduced. The DELPHI collaboration [19] has used a technique in which the mass of the candidate hadronic system is required to be less than M_D; together with additional $b \to u\ell^-\bar{\nu}$ en-

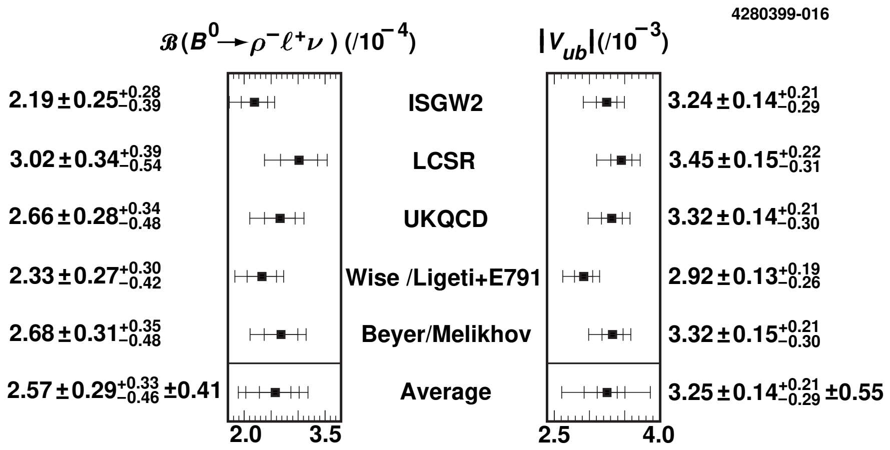

FIGURE 4. CLEO measurement of $B(B^0 \to \rho^- \ell^+ \nu)$ and $|V_{ub}|$. The branching fraction depends on the shapes of kinematic distributions predicted by models through the efficiency of the selection cuts. There is an additional theoretical error on $|V_{ub}|$ due to uncertainty in the overall normalization of form factor predictions.

richment cuts (vertexing, π/K separation), this procedure yields a $b \to u\ell^-\bar{\nu}$ signal of 214 ± 56 events and $B(b \to u\ell^-\bar{\nu}) = (1.57 \pm 0.35 \pm 0.55) \times 10^{-3}$. The LEP Heavy Flavors Working Group has calculated [20] a LEP average value $|V_{ub}|/10^{-3} = 4.04^{+0.41}_{-0.46}(\text{expt})^{+0.43}_{-0.48}(b \to c)^{+0.24}_{-0.25}(b \to u) \pm 0.02(\tau_b) \pm 0.19(\text{HQS})$. Measurements of $|V_{ub}|$ will be an active area of research for years to come!

RARE B DECAYS

With of order 10 M $B\bar{B}$ events recorded, the B-factory experiments are sensitive to decay modes with branching fractions in the range 10^{-6} to 10^{-4}, depending on the number and types of particles produced in the final state and the branching fractions of the daughter particles. With this level of sensitivity, experiments are exploring new channels beyond the $b \to c$ transition, which is responsible for the dominant class of B decays. CLEO has been producing a steady stream of measurements of new rare decay modes (with BaBar and Belle soon to follow), and there is a large theoretical effort to understand and exploit this new information.

The current frontier of rare decays includes at least five different types of modes: (1) $b \to u$ transitions (*e.g.,* $B \to \pi\pi$ and $B \to \rho\pi$), (2) strong (or gluonic) penguin decays (*e.g.,* $B \to K\pi$), (3) electroweak penguin decays (*e.g.,* $B \to K^*\gamma$, $b \to s\gamma$ inclusive, and $B \to K^{(*)}\ell^+\ell^-$), (4) leptonic decays ($B^+ \to \tau^+\nu_\tau$), and (5) $b \to c$ decays that are color suppressed due to so-called internal W emission. We will focus on the first three types of modes below; some useful reviews of penguins and other rare decays are given in the references [21–23].

Penguins were first observed in B decays by CLEO, which discovered [24] the radiative-penguin process $B \to K^*\gamma$ in 1993. This decay involves an internal loop associated with the $b \to tW^- \to s$ transition; the photon, which is distinctive due to its high energy, can be radiated from any of the charged particles. Since $B \to K\gamma$ is forbidden by angular momentum conservation, $B \to K^*\gamma$ is the simplest exclusive mode, and a handful of decays were originally seen in a sample of about 3M $B\bar{B}$ events. With a sample of 9.7M $B\bar{B}$ events, CLEO has updated and extended these measurements [25]

$$\begin{aligned}
B(B^0 \to K^{*0}\gamma) &= (4.55^{+0.72}_{-0.68} \pm 0.34) \times 10^{-5} \\
B(B^+ \to K^{*+}\gamma) &= (3.76^{+0.89}_{-0.83} \pm 0.28) \times 10^{-5} \\
B(B \to K_2^*(1430)\gamma) &= (1.66^{+0.59}_{-0.53} \pm 0.13) \times 10^{-5}.
\end{aligned}$$

The yields are $88.3^{+12.2}_{-11.5}$ events, $36.7^{+8.3}_{-7.6}$ events and $15.9^{+5.7}_{-5.1}$ events. The branching fractions are certainly within the range of theoretical expectations, but, due to the complications of hadronic effects, precise predictions are available only for the inclusive $b \to s\gamma$ (or $B \to X_s\gamma$) decay. After an enormous theoretical effort, the rate for $b \to s\gamma$ has been calculated [26–28] including all next-to-leading order terms, yielding $B(b \to s\gamma) = (3.28 \pm 0.33) \times 10^{-4}$. This value is consistent with measurements from CLEO [29] and ALEPH [30]:

$$\begin{aligned}
B(b \to s\gamma) &= (3.15 \pm 0.35 \pm 0.41) \times 10^{-4} \text{ (CLEO)} \\
B(b \to s\gamma) &= (3.11 \pm 0.80 \pm 0.72) \times 10^{-4} \text{ (ALEPH)}.
\end{aligned}$$

Although the presence of a loop provides some sensitivity to higher mass particles such as SUSY partners, there is currently no evidence for an anomaly in the $b \to s\gamma$ rate.

The role of gluonic penguins in rare hadronic B decays has been a subject of intense interest for several years, and there is now strong evidence that such processes are important in a number of recently observed modes. The decay $B^- \to \bar{K}^0\pi^-$, for example, is naturally explained as a hadronic penguin: it cannot result from a $b \to u$ transition unless final-state interactions convert a $\bar{u}su\bar{u}$ system into a $\bar{u}sd\bar{d}$ system. This explanation is quite unlikely: the penguin amplitude is $\mathcal{O}(\lambda^2)$, while the tree diagram is $\mathcal{O}(\lambda^4)$, where $\lambda = \sin\theta_C$.

The news that gluonic-penguin contributions can be large is not entirely welcome in all cases. In particular, the decay $B^0 \to \pi^+\pi^-$ produces a CP eigenstate, and it appeared at first that this mode would be well suited to the determination of $\sin 2\alpha$ through a measurement of the time-dependent CP asymmetry. However, as Fig. 5 shows, both $b \to u$ tree and gluonic penguin diagrams can contribute to $B^0 \to \pi^+\pi^-$. This complicates the interpretation of the CP-asymmetry measurement, because there are two amplitudes in addition to the mixing amplitude. The quantitative impact of this complication is still not clear, because we do not yet know the relative size of the penguin and tree contributions.

We can, however, make some simple observations. Power counting in λ shows that the $b \to u$ tree process should contribute more to $\bar{B}^0 \to \pi^+\pi^-$ than to $\bar{B}^0 \to K^-\pi^+$, so that if this were the only amplitude present we would expect $B(\bar{B}^0 \to$

$\pi^+\pi^-) \gg B(\bar{B}^0 \to K^-\pi^+)$. (See the upper-left part of Fig. 5.) On the other hand, the penguin process (with intermediate t or c quarks) should contribute more to $\bar{B}^0 \to K^-\pi^+$ than to $\bar{B}^0 \to \pi^+\pi^-$, so $B(\bar{B}^0 \to K^-\pi^+) \gg B(\bar{B}^0 \to \pi^+\pi^-)$ would indicate a large gluonic-penguin contribution.

In a scenario where $B(\bar{B}^0 \to K^-\pi^+) \approx B(\bar{B}^0 \to \pi^+\pi^-)$, we could conclude that $\bar{B}^0 \to K^-\pi^+$ was predominantly penguin and that $\bar{B}^0 \to \pi^+\pi^-$ was predominantly a tree process. That is, the upper-left and lower-right decay diagrams in Fig. 5 must dominate. For, if the $\bar{B}^0 \to K^-\pi^+$ were mainly a tree process, then the $\bar{B}^0 \to \pi^+\pi^-$ tree contribution should be even larger, and we would observe $B(\bar{B}^0 \to \pi^+\pi^-) > B(\bar{B}^0 \to K^-\pi^+)$.

Table 3 lists just a few of the recent measurements [31–33] of hadronic rare modes by CLEO. These data indicate that $B(\bar{B}^0 \to K^-\pi^+)$ is significantly larger than $B(\bar{B}^- \to \pi^+\pi^-)$, so that the penguin contribution to $B^0 \to \pi^+\pi$ may not be negligible. In this case, it may be preferable to measure $\sin 2\alpha$ using the mode $B \to \rho\pi$, where a Dalitz-plot analysis can in principle be used to help understand the penguin contribution [34].

The interference between $b \to u$ tree and penguin diagrams is sensitive to the CKM angle γ, and direct CP violation is a possibility, although it is not possible to predict the values of the required strong phases. Searches for direct CP violation in B decays have so far yielded only limits [35]. There are numerous theoretical efforts [36–40] to better understand the dynamics of these rare decays. As we saw earlier, CP-violating phases can affect the partial decay widths. Using ratios of certain decay widths or the overall pattern of rare decay, constraints have been derived on γ with a varying degree of dependence on models. At present, our understanding of the strong interaction dynamics in these decays is not adequate to push such attempts very far, but this situation may well change over the next few years.

$D^0\bar{D}^0$ MIXING

The phenomenon of particle-antiparticle oscillations, or mixing, has been a powerful source of information on discrete symmetry violation and on particles at higher mass scales. Both $K^0\bar{K}^0$ and $B^0\bar{B}^0$ oscillations occur and have provided rough estimates of the charm and top quark masses, respectively. The Standard Model predictions for $D^0\bar{D}^0$ mixing are well below the current range of sensitivity. There are, however, many non-Standard Model predictions that give much higher mixing rates, and many of these have now been excluded by the new CLEO measurement [41] that I will discuss here.

Oscillations between a pseudoscalar meson P^0 and its antiparticle $\bar{P}^0$ can be described in terms of an effective hamiltonian matrix

$$\mathbf{H} = \begin{pmatrix} H_{11} & H_{12} \\ H_{21} & H_{22} \end{pmatrix} = \begin{pmatrix} M & M_{12} \\ M_{12}^* & M \end{pmatrix} - \frac{i}{2} \begin{pmatrix} \Gamma & \Gamma_{12} \\ \Gamma_{12}^* & \Gamma \end{pmatrix}.$$

TABLE 3. Selection of results [31–33] on hadronic rare B decays from CLEO. Limits are given at 90% C.L. The yields for modes with η or η' mesons are given separately for each final state reconstructed in Ref. [33].

Mode	$N_{\rm SIG}$	Signif. (σ)	$\mathcal{B}/10^{-6}$
$\pi^+\pi^-$	$20.0^{+7.7}_{-6.5}$	4.2	$4.3^{+1.6}_{-1.4} \pm 0.5$
$\pi^+\pi^0$	$21.3^{+9.7}_{-8.5}$	3.2	< 12.7
$K^\pm\pi^\mp$	$80.2^{+11.8}_{-11.0}$	11.7	$17.2^{+2.5}_{-2.4} \pm 1.2$
$K^\pm\pi^0$	$42.1^{+10.9}_{-9.9}$	6.1	$11.6^{+3.0+1.4}_{-2.7-1.3}$
$K^0\pi^\pm$	$25.2^{+6.4}_{-5.6}$	7.6	$18.2^{+4.6}_{-4.0} \pm 1.6$
$K^0\pi^0$	$16.1^{+5.9}_{-5.0}$	4.9	$14.6^{+5.9+2.4}_{-5.1-3.3}$
$B^- \to \pi^-\rho^0$	$29.8^{+9.3}_{-9.6}$	5.4	$10.4^{+3.3}_{-3.4} \pm 2.1$
$\bar{B}^0 \to \pi^\pm\rho^\mp$	$31.0^{+9.4}_{-8.3}$	5.6	$27.6^{+8.4}_{-7.4} \pm 4.2$
$B^- \to \pi^-\omega$	$28.5^{+8.2}_{-7.3}$	6.2	$11.3^{+3.3}_{-2.9} \pm 1.4$
$B^- \to K^-\rho^0$	$22.4^{+10.7}_{-9.1}$	3.7	< 17
$B^- \to \pi^-\bar{K}^{*0}$	$13.4^{6.2}_{-5.2}$	3.6	< 16
$\bar{B}^0 \to K^\pm\rho^\mp$	$16.4^{+7.8}_{-6.6}$	3.5	< 32
$\bar{B}^0 \to \pi^0\bar{K}^{*0}$	$0.0^{+3.0}_{-0.0}$	0.0	< 3.6
$B^+ \to \eta' K^+$		16.8	$80^{+10}_{-9} \pm 7$
$B^0 \to \eta' K^0$		11.7	$89^{+18}_{-16} \pm 9$
$B^+ \to \eta K^{*+}$		4.8	$26.4^{+9.6}_{-8.2} \pm 3.3$
$B^0 \to \eta K^{*0}$		5.1	$13.8^{+5.5}_{-4.6} \pm 1.6$

By diagonalizing $\mathbf{H}$, we obtain the mass eigenstates as linear combinations of the two original basis states, P^0 and $\bar{P}^0$. The masses and lifetimes of these physical states are different; in the absence of CP violation these splittings are given by $\Delta M = \pm 2|M_{12}|$ and $\Delta\Gamma = \pm 2|\Gamma_{12}|$.

The elements of the mass matrix (M_{ij}) and the decay matrix (Γ_{ij}) describe distinctive classes of transitions between P^0 and $\bar{P}^0$: Γ_{12} is the amplitude for $\bar{P}^0 \to f \to P^0$ via on-shell intermediate states, while M_{12} describes transitions through off-shell, or virtual, intermediate states. The on-shell states are those that both P^0 and $\bar{P}^0$ can decay into, while off-shell states provide the sensitivity to physics at high mass scales. CP violation in mixing can arise from the inteference between on-shell and off-shell amplitudes, leading to $\Gamma(P^0 \to \bar{P}^0) \neq \Gamma(\bar{P}^0 \to P^0)$. This occurs when $M_{12} - \frac{i}{2}\Gamma_{12} \neq M^*_{12} - \frac{i}{2}\Gamma^*_{12}$. The dimensionless quantities $x = 2M_{12}/\Gamma$ and $y = \Gamma_{12}/\Gamma$ are commonly defined and we will use them below.

The process used to study mixing in CLEO is $e^+e^- \to c\bar{c}$, where the charm or anticharm quark fragments into a D^*: $c \to D^{*+} \to D^0\pi^+_s$. The charge of the "soft-pion" π^+_s accompanying the D^0 is used to determine whether the intial state is D^0 or $\bar{D}^0$. In this analysis, neutral D mesons are reconstructed in $K^-\pi^+$ and $K^+\pi^-$ final states, so the normal Cabibbo-favored $D^0 \to K^-\pi^+$ decay produces an opposite-sign $\pi^+_s K^-$ charge correlation. If mixing occurs, $D^0 \to \bar{D}^0 \to K^+\pi^-$, it produces the "wrong-sign" charge correlation ($\pi^+_s K^+$). However, the direct doubly Cabibbo-suppressed decay (DCSD) $D^0 \to K^+\pi^-$ also gives this charge correlation

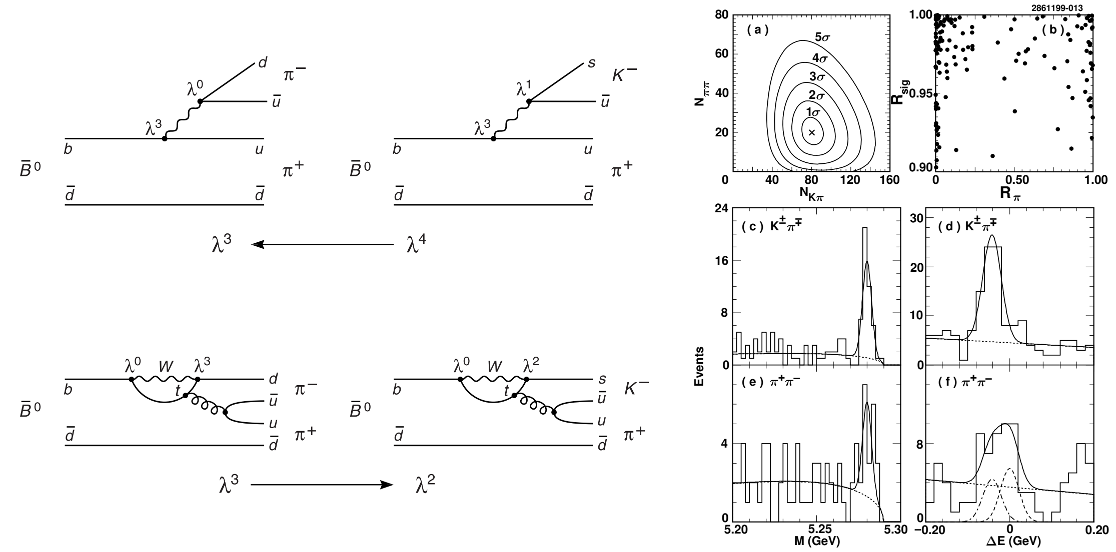

FIGURE 5. Left: Diagrams for $\bar{B}^0 \to \pi^+\pi^-$ and $\bar{B}^0 \to K^-\pi^+$. Both modes have contributions from tree $b \to u$ and penguin processes. The figure shows the dependence of each amplitude on $\lambda = \sin\theta_C$, as determined from the Wolfenstein parametrization of the CKM matrix. The figures at right show results from a recent analysis of $B \to \pi^+\pi^-$ and $B \to K^-\pi^+$. (a) shows the likelihood contours as a function of the number of $K\pi$ and $\pi\pi$ events, while (b) shows an event-by-event probability for an event to be signal (either $\pi\pi$ or $K\pi$ vs. the probability to be a $\pi\pi$ event. Signals are seen for these modes in the reconstructed B mass (c, e) and in the ΔE distributions (d, f), which compare the reconstructed energy to the expected energy (beam energy).

$(\pi_s^+ K^+)$, and it is distinguished from mixing using the decay time-dependence as described below. Semileptonic final states do not suffer from this ambiguity, but they have larger backgrounds and will be the subject of a future analysis.

Figure 6 shows the signal for the wrong-sign charge correlated events. Under the assumption of no mixing, this signal ($44.8^{+9.7}_{-8.7}$ events) leads to a wrong-sign fraction

$$R = \frac{\Gamma(D^0 \to K^+\pi^-)}{\Gamma(D^0 \to K^-\pi^+)} = (0.332^{+0.063}_{-0.065} \pm 0.040)\%, \tag{10}$$

which is substantially more precise than the previous PDG value $R = (0.72 \pm 0.25)\%$.

To distinguish a potential mixing signal from DCSD decay, CLEO measures the wrong-sign rate as a function of the decay time, which can be determined from the distance between the D^0 production point and its decay vertex. In CLEO, this measurement is performed using a three-layer silicon vertex detector that surrounds the beam-pipe. The innermost layer of this device is only 2.35 cm from the beam axis, and the very small vertical size of the beam spot ($\sigma_y \approx 7\ \mu$m) provides a good constraint on the D^0 production vertex. The wrong-sign rate is given by

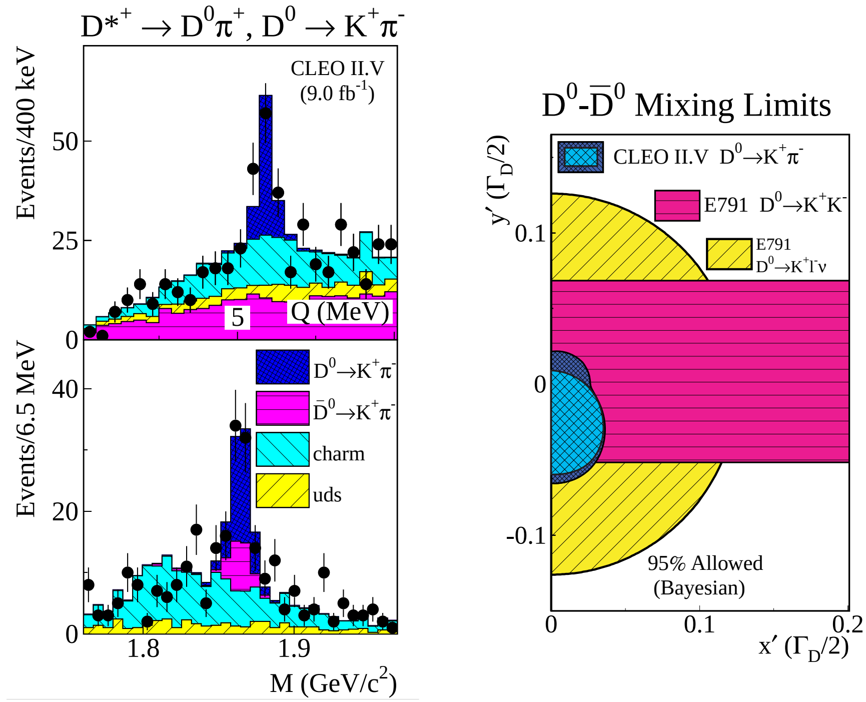

FIGURE 6. $D^0\bar{D}^0$ mixing results from CLEO. Left: data from the wrong-sign correlated events showing a signal corresponding to the D^{*+} decay (above) and the D^0 decay below. These are time-integrated signals; to distinguish between doubly Cabibbo suppressed decay and mixing CLEO analyzes the time dependence of the decay. Right: $D^0\bar{D}^0$ mixing limits from CLEO and Fermilab E791.

$$r_{ws}(t) = (R_D + \sqrt{R_D}y't + \frac{1}{4}(x'^2 + y'^2)t^2)e^{-t}, \tag{11}$$

where the decay time t is measurement expressed in units of the D^0 proper lifetime and R_D is the DCSD rate relative to the Cabibbo-favored rate. The quantities x' and y' in the equation allow for a possible strong phase δ between the Cabibbo-favored and the DCSD amplitudes: $x' = x\cos\delta + y\sin\delta$ and $y' = y\cos\delta - x\sin\delta$.

The fit to the proper lifetime distribution gives $x' = (0.0 \pm 1.5 \pm 0.2)\%$, or $|x'| < 2.9\%$ at 95% C.L. ($(1/2)x'^2 < 0.041\%$), and $y' = (-2.5^{+1.4}_{-1.6} \pm 0.3)\%$, or $-5.8\% < y' < 1.0\%$ at 95% C.L. Although there is no statistically significant indication for mixing, these limits are substantially more sensitive than previous results. Figure 6 shows the allowed region in the x'-y' plane. A extensive compilation of non-Standard Model $D^0\bar{D}^0$ mixing predictions shows [42] that many are excluded by these new limits. $D^0\bar{D}^0$ mixing studies are also now being performed by the FOCUS experiment [43].

TIME-DEPENDENT CP ASYMMETRIES FROM THE INTERFERENCE BETWEEN MIXING AND DECAY

The measurement of time-dependent CP asymmetries is the main goal of the new asymmetric-energy e^+e^- colliders PEP-II and KEKB, and their associated detectors, BaBar and Belle. The mechanism generating the interference was shown in Fig. 1: the processes $B^0 \to f$ and $B^0 \to \bar{B}^0 \to f$ can interfere, giving sensitivity to their relative phases. The final state f, which must be reachable from both B^0 and $\bar{B}^0$, can be an eigenstate of CP ($f = f_{CP}$), with eigenvalue η_{CP}. The measured asymmetry is defined by

$$\mathcal{A}_{\mathcal{CP}} = \frac{\Gamma(B^0(t) \to f_{CP}) - \Gamma(\bar{B}^0(t) \to f_{CP})}{\Gamma(B^0(t) \to f_{CP}) + \Gamma(\bar{B}^0(t) \to f_{CP})}. \tag{12}$$

To measure the two rates as a function of time, one must be able to carry out the following procedure:

1. Reconstruct a sufficient number of B^0 or $\bar{B}^0$ decays in the final state f_{CP}. Examples of such final states are $J/\psi K_s^0$, $J/\psi K_L^0$, and $\pi^+\pi^-$.
2. Determine whether the meson was a B^0 or $\bar{B}^0$ at some well-defined reference time. Tagging the B flavor relies on measurements of particles produced in association with the B meson. At the $\Upsilon(4S)$, the initial system is $B^0\bar{B}^0$, and it evolves coherently until one of the B mesons decays. To a large extent, tagging relies on inclusive semileptonic decays ($b \to \ell^-$, $\bar{b} \to \ell^+$), in which the lepton charge is correlated with the B-meson flavor, and inclusive charge kaon production ($\bar{B}^0 \to D \to K^-$, $B^0 \to \bar{D} \to K^+$). For each tagging method, the mistag fraction must be carefully evaluated.
3. Measure the proper time interval between the decay time for $B^0(\bar{B}^0) \to f_{CP}$ and the reference time at which the flavor of the $B^0(\bar{B}^0)$ meson is tagged.

These three requirements place strong demands on both the accelerator and the detector. Figure 7 shows an example of the difference in decay rate vs. time for mesons that are initially B^0 and $\bar{B}^0$. The figure is limited to positive decay times, which means that the tag decay occurs prior to the decay to the CP eigenstate. If the time order of the two is reversed, it turns out that the asymmetry reverses sign as a consequence of Bose statistics and the p-wave nature of the $\Upsilon(4S)$ decay. If the decay time is not measured, the numerator in Eq. 12 integrates to zero, and there is no observable asymmetry! Measurement of the decay time is mandatory at the $\Upsilon(4S)$, while in other environments, *e.g.*, hadron colliders, it is desirable but not strictly essential.

To determine the difference in decay time between the two neutral B mesons, one must measure the spatial separation between their decay vertices. The B mesons are produced nearly at rest in the $\Upsilon(4S)$ frame, so the $B\bar{B}$ system must be boosted relative to the detector frame. It is this requirement that has led to the enormous

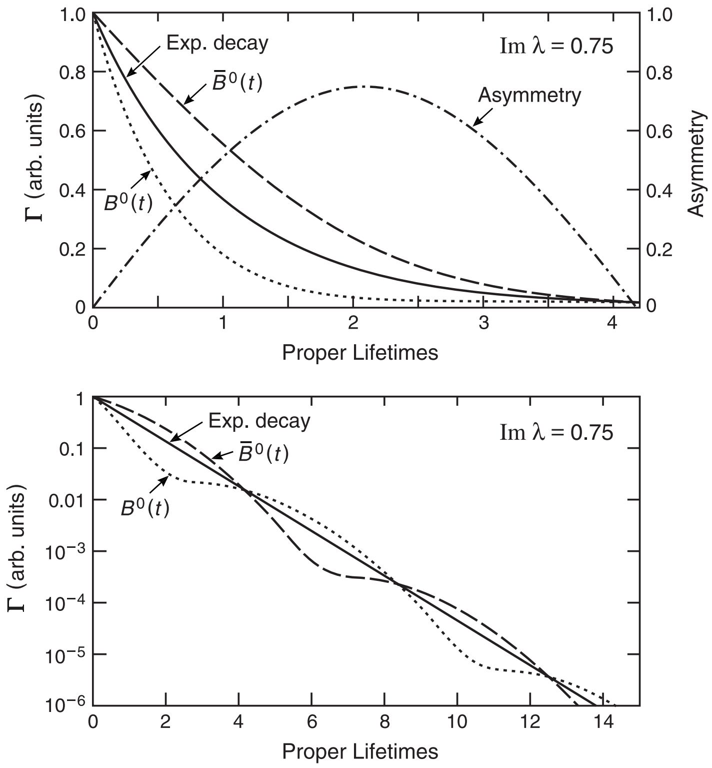

FIGURE 7. Example of a CP asymmetry resulting from the interference between B^0 mixing and decay as a function of proper lifetime. The size of the asymmetry is chosen arbitrarily but is consistent with some predictions for $\sin 2\beta$ based on the Standard Model and constraints from other measurements in B and K physics. Note that CP violation leads to a non-exponential decay.

effort of building asymmetric energy e^+e^- colliders. The unequal beam energies mean that the $\Upsilon(4S)$ has the boost $\beta\gamma = (E_{e^-} - E_{e^+})/2E_{e^-}E_{e^+}$, so the mean vertex separation is $\Delta z = \beta\gamma c < \Delta t > \approx 260\ \mu$m, since $< \Delta t > = \tau_B = 1.6$ ps. This is a much smaller distance scale than in kaon physics experiments, and it means that high-precision silicon strip vertex detectors play a large role in these measurements. The need for efficient tagging with a relatively low mistag rate implies that these experiments need good electron and muon identification and good π/K separation.

Figure 8 shows preliminary results obtained by Belle and BaBar that help to build an understanding of the detector systems needed to measure time-dependent CP asymmetries. The Belle data show their first measurement of the B^0 lifetime, while the BaBar data show a $B^0\bar{B}^0$ oscillation measurement using dilepton events. We can expect first results on CP asymmetries later this summer, but precision measurements will need to await more data.

With major e^+e^- and hadron-collider facilities coming on line, heavy-quark physics has a very bright future. At the next CIPANP meeting in three years, there should be enormous number of new results!

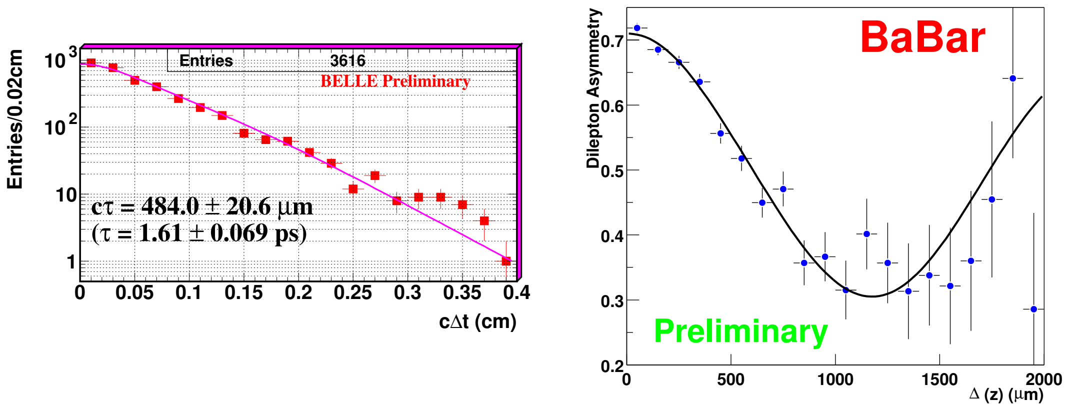

FIGURE 8. Progress from Belle and BaBar. Left: a preliminary measurement of the B lifetime from Belle; right: a preliminary of $B^0\bar{B}^0$ mixing from BaBar.

ACKNOWLEDGEMENTS

Many people provided valuable information that helped greatly in the preparation of this talk. It is a pleasure to thank Leo Piilonen from Belle and David Jaffe, Karl Ecklund, David Asner, Harry Nelson, and David Rubin from CLEO. I would also like to thank the conference organizers for a stimulating and collegial conference.

REFERENCES

1. B. Wicklund, Plenary Session talk at this conference.
2. R. Mohapatra, Plenary Session talk at this conference.
3. A. El-Khadra, Plenary Session talk at this conference.
4. J.H. Christenson, J.W. Cronin, V.L. Fitch, and R. Turlay, Phys. Rev. Lett. **13**, 138 (1964).
5. J.W. Cronin, Rev. Mod. Phys. **53**, 373 (1981).
6. Y. Nir, in *Proceedings of the Twentieth SLAC Summer Institute on Particle Physics: The Third Family and the Physics of Flavor*, Stanford, CA, July 13–24, 1992, SLAC-412.
7. A pedagogical discussion of CP violation and other aspects of B physics is contained in J.D. Richman, *Heavy Quark and CP Violation,* in *Probing the Standard Model of Particle Interactions*, Les Houches Session LXVIII, 28 July–5 September, 1997 (Elsevier, Amsterdam, 1999), ed. R.Gupta, A. Morel, E. De Rafael, and F. David, http://hep.ucsb.edu/driver/driver_houches12.ps (preprint).
8. M. Neubert, Phys. Rep. **245**, 259 (1994).
9. *Review of Particle Physics*, Eur. Phys. J. C 15, 1 (2000).
10. BaBar Physics Book, P.F. Harrison and H.R. Quinn eds., SLAC-R-504 (1998).
11. J.E. Duboscq *et al.* (CLEO), Phys. Rev. Lett. **76**, 3898 (1996).

12. J. Bartelt *et al.* (CLEO), Phys. Rev. Lett. **82**, 3746 (1999).
13. J.P. Alexander *et al.*, CLEO CONF 00-03, ICHEP00 770, Submitted to XXXth International Conference on High Energy Physics, July 2000, Osaka, Japan.
14. G. Abbiendi *et al.* (OPAL), CERN-EP-2000-032, Phys. Lett. B482, 15 (2000).
15. J.D. Richman and P.R. Burchat, Rev. Mod. Phys. **67**, 893 (1995).
16. L. Gibbons and K. Honscheid, in *Review of Particle Physics*, Eur. Phys. J. C 15, 581 (2000).
17. B.H. Behrens *et al.* (CLEO), Phys. Rev. D **61**, 052001 (2000).
18. J.P. Alexander, *et al.* (CLEO), Phys. Rev. Lett **77**, 5000 (1996).
19. P. Abreu *et al.* (DELPHI), CERN-EP-2000-030, submitted to Phys. Lett. B
20. Heavy Flavor Working Group, LEPHFS note 99-02, March 2000, and references therein.
21. A.J. Buras, Les Houches Lectures, in *Probing the Standard Model of Particle Interactions*, Les Houches Session LXVIII, 28 July–5 September, 1997 (Elsevier, Amsterdam, 1999), ed. R.Gupta, A. Morel, E. De Rafael, and F. David, hep/ph-9806471.
22. K. Lingel, T. Skwarnicki, J.G. Smith, Ann. Rev. Nucl. Part. Sci. **48**, 253 (1998).
23. A. Vainshtein, Int. J. Mod. Phys. A14, 4705 (1999).
24. R. Ammar *et al.* (CLEO), Phys. Rev. Lett. **71**, 674 (1993).
25. T.E. Coan *et al.* (CLEO), Phys. Rev. Lett. **84**, 5283 (2000).
26. K. Chetyrkin, M. Misiak, and M. Münz, Phys. Lett. B**400**, 206 (1997); Erratum–ibid., Phys. Lett. B**425**, 414 (1998).
27. A.J. Buras, A. Kwiatkowski and N. Pott, Phys. Lett. **B414**, 157 (1997); Erratum–ibid., Phys. Lett. **B434**, 459 (1998).
28. A.L. Kagan and Matthias Neubert, Eur. Phys. J. **C7**, 5 (1999).
29. S. Glenn *et al.* (CLEO), CLEO-CONF-98-17, submitted to the International Conference on High Energy Physics, Vancouver, Canada, 1998.
30. R. Barate *et al.* (ALEPH), Phys. Lett. B **429**, 169 (1998).
31. D. Cronin-Hennessy *et al.*, preprint CLNS-99-1650, hep-ex/0001010, submitted to Phys. Rev. Lett.
32. C.P. Jessop *et al.* (CLEO), preprint CLNS-99-1652, hep-ex/0006008, submitted to Phys. Rev. Lett.
33. S.J. Richichi *et al.* (CLEO), Phys. Rev. Lett. **85**, 520 (2000).
34. A.E. Snyder and H.R. Quinn, Phys. Rev. D **48**, 2139 (1993).
35. S. Chen *et al.* (CLEO), Phys. Rev. Lett. **85**, 525 (2000).
36. A. Ali, G. Kramer, C.D. Lu, Phys. Rev. D**58**, 094009 (1998).
37. A. Ali, G. Kramer, C.D. Lu, Phys. Rev. D**59**, 014005 (1999).
38. M. Beneke, G. Buchalla, M. Neubert, C.T. Sachrajda, hep-ph/0006124.
39. W.-S. Hou, J.G. Smith, F. Würthwein, hep-ex/9910014.
40. Y.-H. Chen, H.-Y. Cheng, B. Tseng, and K.-C. Yang, Phys. Rev. D **60**, 094014 (1999); hep-ph/9903453 v2.
41. R. Godang *et al.* (CLEO), Phys. Rev. Lett. **84**, 5038 (2000).
42. H.N. Nelson, submitted to the 1999 Lepton-Photon Symposium, hep-ex/9908021 (unpublished).
43. P. Sheldon, parallel session talk at this conference.